Compromised fidelity of endocytic synaptic vesicle protein sorting in the absence of stonin 2

Natalia L. Kononenko[a,b], M. Kasim Diril[c], Dmytro Puchkov[a], Michael Kintscher[b], Seong Joo Koo[a], Gerit Pfuhl[d], York Winter[d], Martin Wienisch[e], Jürgen Klingauf[e], Jörg Breustedt[b], Dietmar Schmitz[b], Tanja Maritzen[a,1,2], and Volker Haucke[a,b,c,1,2]

[a]Department of Molecular Pharmacology and Cell Biology, Leibniz Institut für Molekulare Pharmakologie, 13125 Berlin, Germany; [b]NeuroCure Cluster of Excellence, Charité Berlin, 10117 Berlin, Germany; [c]Freie Universität Berlin, Institut für Chemie und Biochemie, 14195 Berlin, Germany; [d]Department of Cognitive Neurobiology, Humboldt Universität zu Berlin, 10117 Berlin, Germany; and [e]Institute for Medical Physics and Biophysics, University of Münster, 48149 Münster, Germany

Edited by Pietro De Camilli, Yale University and Howard Hughes Medical Institute, New Haven, CT, and approved December 28, 2012 (received for review October 23, 2012)

Neurotransmission depends on the exocytic fusion of synaptic vesicles (SVs) and their subsequent reformation either by clathrin-mediated endocytosis or budding from bulk endosomes. How synapses are able to rapidly recycle SVs to maintain SV pool size, yet preserve their compositional identity, is poorly understood. We demonstrate that deletion of the endocytic adaptor stonin 2 (Stn2) in mice compromises the fidelity of SV protein sorting, whereas the apparent speed of SV retrieval is increased. Loss of Stn2 leads to selective missorting of synaptotagmin 1 to the neuronal surface, an elevated SV pool size, and accelerated SV protein endocytosis. The latter phenotype is mimicked by overexpression of endocytosis-defective variants of synaptotagmin 1. Increased speed of SV protein retrieval in the absence of Stn2 correlates with an up-regulation of SV reformation from bulk endosomes. Our results are consistent with a model whereby Stn2 is required to preserve SV protein composition but is dispensable for maintaining the speed of SV recycling.

pHluorin | hippocampus | mossy fibers

Neurotransmission involves the calcium-regulated fusion of synaptic vesicles (SVs), a process that requires the SV calcium sensor synaptotagmin (Syt) (1) and components of the active zone (AZ) that define sites of neurotransmitter release (2). Post-exocytic fusion SV membranes are retrieved by endocytosis from the plasma membrane (2–5) to regenerate SVs of the correct size and composition (6). Alternatively, SVs can also be reformed from large plasma membrane infoldings and from endosomes (7) via a brefeldin A–sensitive pathway (8) that may become particularly important under conditions of sustained high-level activity and involves endosomal adaptor complexes such as adaptor protein complex 1 (AP-1) (9, 10). Maintenance of the SV pool requires that the number of recycled SVs closely matches those having undergone exocytosis. As SVs are characterized by a precise protein composition (11) that at least for some SV proteins including Syt1, VGLUT1, and SV2A displays little intervesicle variation (12), molecular mechanisms must exist to control the fidelity of SV protein sorting while maintaining the speed of exo-endocytosis.

The mechanisms by which exo-endocytic balance and the fidelity of SV protein sorting are maintained are unknown. One possibility is that retrieval of SV proteins involves clustering (13, 14), which would alleviate a need for specific sorting, even if multiple pathways of SV reformation are used (9, 10). However, data based on imaging of SV proteins tagged with the GFP-derived pH sensor pHluorin indicate that exocytosed and newly endocytosed SV proteins are not identical, suggesting that intermixing between exocytosed and preexisting surface pools of vesicle proteins occurs (15, 16). If SVs lose their identity over multiple rounds of exo-endocytosis, specific mechanisms should exist for the cargo-specific recognition and sorting of SV proteins, e.g., by adaptors (4, 15).

Several components of the endocytic machinery may function as adaptors for SV protein sorting. These components include the heterotetrameric adaptor complex AP-2, a key component of the clathrin machinery involved in sorting of constitutive cargo in nonneuronal cells (17), AP180, an abundant factor of synaptic clathrin-coated vesicles (18–20), the BAR-SH3 domain protein endophilin (8, 21), and the AP-2μ–related protein stonin 2 (Stn2), a binding partner of the SV calcium sensor synaptotagmin (22–24). AP180 together with its ubiquitously expressed paralog Clathrin Assembly Lymphoid Myeloid Leukemia Protein (CALM) has been proposed to facilitate sorting of the SV SNARE synaptobrevin 2 (19), whereas endophilin may regulate the speed of vesicular glutamate transporter 1 (VGLUT1) retrieval (8). Genetic studies have been inconclusive with respect to the mechanisms of SV protein sorting because all adaptor mutants studied thus far exhibit generalized defects in SV endocytosis (4, 5) leading to gross alterations in synapse structure and functionality. For example, loss of AP-2 is associated with early embryonic lethality in mice (25), whereas mouse mutants lacking endophilin A are perinatally lethal due to strongly impaired synaptic transmission (21).

Conflicting data exist regarding the physiological function of stonins in vivo: knockdown studies in transfected neurons (26) and data from invertebrates suggest a general essential role of

Significance

Brain function depends on neurotransmission, and alterations in this process are linked to neuropsychiatric disorders. Neurotransmitter release requires the rapid recycling of synaptic vesicles (SVs) by endocytosis. How synapses can rapidly regenerate SVs, yet preserve their molecular composition, is poorly understood. We demonstrate that mice lacking the endocytic protein stonin 2 (Stn2) show changes in exploratory behavior and defects in SV composition, whereas the speed at which SVs are regenerated is increased. As Stn2 is implicated in schizophrenia and autism in humans, our findings bear implications for neuropsychiatric disorders.

Author contributions: N.L.K., M.K.D., D.P., M.K., G.P., Y.W., J.K., J.B., D.S., T.M., and V.H. designed research; N.L.K., D.P., M.K., S.J.K., G.P., M.W., J.B., and T.M. performed research; M.K.D., S.J.K., and J.K. contributed new reagents/analytic tools; N.L.K., M.K.D., D.P., M.K., S.J.K., G.P., Y.W., M.W., J.K., J.B., D.S., and T.M. analyzed data; and N.L.K., D.S., and V.H. wrote the paper.

The authors declare no conflict of interest.

This article is a PNAS Direct Submission.

Freely available online through the PNAS open access option.

[1]T.M. and V.H. contributed equally to this work.

[2]To whom correspondence may be addressed. E-mail: tmaritzen@googlemail.com or haucke@fmp-berlin.de.

This article contains supporting information online at www.pnas.org/lookup/suppl/doi:10.1073/pnas.1218432110/-/DCSupplemental.

stonins (termed Stn2 in mammals, stoned B in *Drosophila melanogaster*, and unc-41 in *Caenorhabditis elegans*) in SV endocytosis, which is evidenced by a reduced SV pool size and impaired neurotransmission in loss-of-function alleles (27–31). On the other hand, the evolutionary conserved association of stonins with the endocytic machinery and with Syt (22–24) has been taken as evidence in favor of a more specific role of Stn2 in Syt sorting, although this postulate has never been tested at the organismic level in mammals in vivo.

Here we demonstrate that deletion of Stn2 in mice compromises the fidelity of SV protein sorting, whereas the apparent speed of SV retrieval is increased. Loss of Stn2 leads to selective missorting of synaptotagmin 1 (Syt1) to the neuronal surface, an elevated SV pool size, and accelerated SV endocytosis. The latter phenotype is mimicked by overexpression of endocytosis-defective variants of Syt1. Increased speed of SV protein retrieval in the absence of Stn2 correlates with an up-regulation of SV reformation from bulk endosomes. Our results are consistent with a model according to which Stn2 is required to preserve SV protein composition but is dispensable for maintaining the speed of SV recycling.

Results

Increased SV Pool Size and Altered Short-Term Plasticity in the Absence of Stn2. To address the question of whether and how the fidelity of SV protein sorting may be linked to the speed of retrieval of SV membranes, we focused on Stn2, the mammalian homolog of *Drosophila* stoned B(27, 30) and of *C. elegans* unc-41 (24, 31). As the function of Stn2 in the mammalian nervous system in vivo has not been explored, we generated Stn2 KO mice (Fig. S1*A*). Unlike their invertebrate counterparts (24) Stn2 KO mice were viable and fertile (Fig. S1 *B* and *C*) and displayed no gross alterations in brain anatomy or synapse density at birth (see below and Figs. S5 and S6). The bulk levels of exo-endocytic proteins in brain homogenates were also unaltered (Fig. S1 *D* and *E*), indicating that Stn2, unlike its invertebrate homologs, is not required for viability. Importantly, no compensation by Stn1 (the only other mammalian stonin) was observed, which is not expressed in CNS neurons.

Stn2 is expressed at the highest levels in the hippocampus (Fig. S2*Ai*), with a strong increase in expression during the first 2 wk of postnatal development (Fig. S2*Aii*). Within the hippocampus, Stn2 is most highly expressed at hippocampal mossy fiber (MF) terminals (Fig. S2 *B* and *C*). We therefore performed ultrastructural analysis of MF synapses from adult WT and Stn2 KO mice using electron microscopy. Surprisingly, MF terminals from Stn2 KO mice displayed a significant increase in the number of SVs (Fig. 1 *A*–*C*; Table S1), whereas other parameters such as the number of docked SVs and the size and number of AZs were unaltered (Table S1). This phenotype differs strikingly from the depletion of SVs observed in mice or flies lacking other endocytic proteins (4, 5, 21, 32) or stonin in invertebrates (27, 29, 31).

To determine whether the elevated SV pool observed at Stn2 KO synapses was functional and to probe for possible alterations in neurotransmission, we analyzed MF synapses in acute hippocampal brain slices from WT and Stn2 KO mice by electrophysiology. Stn2-deficient MF synapses displayed significant differences in short-term plasticity (Fig. 1 *D*–*J*). This difference was evidenced by enhanced paired pulse facilitation (Fig. 1 *D* and *E*) and frequency facilitation (Fig. 1 *F*–*H*), a paradigm where following baseline stimulation at 0.05 Hz, the stimulation frequency is raised to 1 Hz for 20 pulses and then turned back to baseline. As changes in SV pool size and/or in the rate of SV recycling may become overt during high-frequency firing, we also analyzed the responses of MF synapses from Stn2 KO mice to sustained stimulation at 33 Hz. Trains of action potentials (APs) evoked a transient enhancement of transmission during the initial phase of the train and a lower, albeit greater, than baseline steady-state level in slices from both WT and Stn2 KO mice (Fig. 1*I*). Significantly higher responses were elicited in slices from Stn2 KO mice during the steady-state phase (Fig. 1*J*) in striking contrast to the depression seen in other endocytic mutants (4, 21, 32). Thus, loss of Stn2 leads to increased short-term facilitation, likely reflecting a reduced release probability of MF synapses and a partial resistance of KO synapses to high frequency–induced depression.

Synaptic plasticity and hippocampal function have been linked to exploratory behavior (33), with a particularly important role for dentate granule cells and the MF pathway in exploratory learning (34). In agreement with the observed changes in MF short-term plasticity, Stn2 KO mice displayed increased explorative activity in the open arena (Fig. S3*A*), as well as increased vertical locomotion (Fig. S3*B*), whereas spontaneous alternation performance in the Y-maze, considered as a test for working memory, did not differ significantly (Fig. S3*D*). Moreover, Stn2 KO mice had a shorter latency to approach a new object than WT mice (Fig. S3*C*). The increased explorative drive in Stn2 KO mice was not due to reduced anxiety or fear (Fig. S3 *F* and *G*), consistent with their unaltered behavior in the dark-light box (Fig. S3*E*). Stn2 KO mice also did not display memory deficits in object habituation experiments (Fig. S3*H*). Thus, loss of Stn2 causes increased locomotion- and exploration-related behaviors in mice. This phenotype resembles arousal seeking and impulsivity observed in patients suffering from Tourette syndrome (35) or schizophrenia (36), which are neuropsychiatric disorders linked to mutations in Stn2 in humans (37, 38).

Collectively, our results indicate that loss of Stn2 leads to increased short-term facilitation and to a partial resistance to high frequency–induced depression, consistent with an elevated SV pool size (Fig. 1 *A*–*C*). These phenotypic changes correlate with increased exploration-related behaviors in Stn2 KO mice and radically differ from those of other endocytic protein mutants described thus far (4, 21, 32). We thus decided to unravel the molecular mechanisms underlying this phenotype in detail.

Repartitioning of Syt1 to the Neuronal Surface in Stn2 KO Brains. Stn2 has been postulated to selectively associate with Syt1 (22, 23) but not with other SV proteins such as synaptophysin (Syp), synaptobrevin 2 (Syb2), or VGLUT1. We confirmed this by conducting coimmunoprecipitation experiments from brain lysates of WT or Stn2 KO mice using antibodies against Stn2 (Fig. S4*A*). Moreover, Stn2 specifically associated with Syt1 but not with Syp, Syb2, or VGLUT1 in HEK293 cells expressing either SV protein alone (Fig. S4*B*) or in pairwise combinations (Fig. S4*C*). As Syt1 has also been reported to associate with AP-2 (39), presumably in a tripartite complex with Stn2 (23), we also probed the association of Syt1 with these endocytic proteins by immunoprecipitation from native tissue lysates. As expected, Syt1 was found to associate with both AP-2 and Stn2 in lysates from WT mice. By contrast, Syt1 was absent from anti–AP-2 or anti-Stn2 immunoprecipitates derived from Stn2 KO mice (Fig. 2*A*), indicating that Stn2 is required for complex formation between AP-2 and Syt1. Thus, Stn2 specifically associates with Syt1 but not with other SV proteins and is required for linking Syt1 to the clathrin-based endocytic machinery, supporting a cargo-selective function of Stn2 in SV endocytosis.

If this was the case, one would expect alterations in the distribution of Syt1 due to a compromised fidelity of sorting in the absence of Stn2. To address this, we first analyzed the expression level of Syt1 in brain sections from WT or Stn2 KO mice. Total Syt1 levels were slightly reduced in hippocampal sections from 6-wk-old (87.9 ± 10.6% of WT) and significantly decreased from 1.5-y-old (74.2 ± 5.7% of WT) KO animals (Fig. 2 *B* and *C*). Decreased hippocampal expression was also observed for the direct Stn2 binding partner AP-2 and for clathrin, whereas expression of synaptobrevin 2 (Syb2) remained unchanged (Fig.

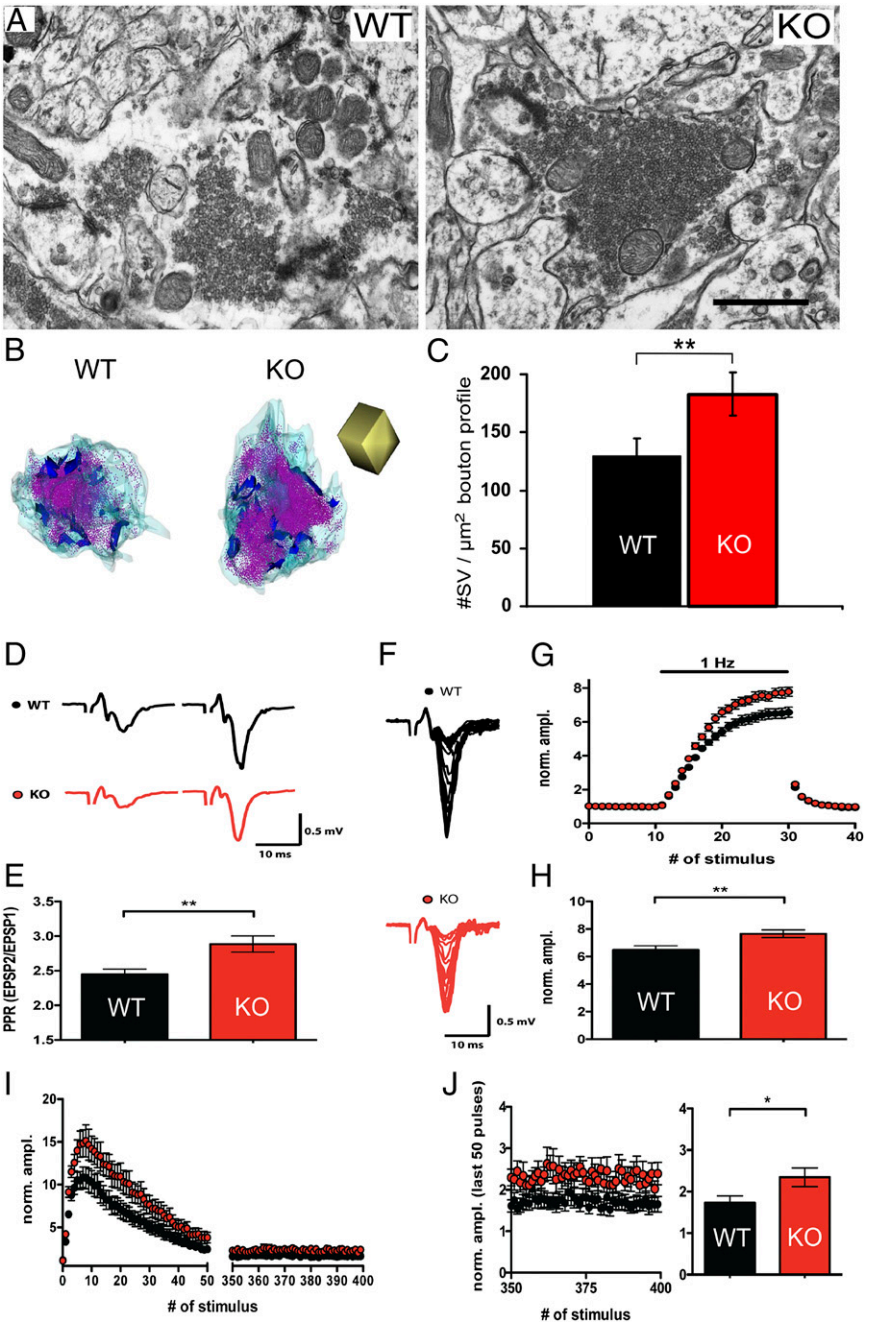

Fig. 1. Increased SV pool size and altered short-term plasticity in the absence of Stn2. (*A*) Electron micrographs of WT and KO MF terminals. (Scale bar, 1 µm.) (*B*) 3D reconstructions of WT and KO MF terminals: SVs, magenta; cyan, presynaptic membrane; blue, postsynaptic membranes. Cube, 1 × 1 × 1 µm. (*C*) Mean SV density in WT and Stn2 KO synapses (40 synapses per genotype, $^{**}P < 0.01$). (Scale bar, 1 µm.) (*D–J*) MF short-term plasticity is increased in Stn2 KO mice. (*D*) Representative traces of paired-pulse ratio (PPR) with interstimulus interval of 50 ms for WT and KO. PPR quantification is shown in *E* (second/first pulse, WT-PPR:2.5 ± 0.08, $n = 10$ slices, vs. KO-PPR:2.9 ± 0.1, $n = 11$ slices, $^{*}P < 0.01$). (*F*) Frequency facilitation (FF) of MF responses in WT and KO slices. Normalized amplitudes of fEPSPs are depicted in *G*. (*H*) Quantification of averaged last five pulses during 1-Hz stimulation (WT-FF: 6.5 ± 0.3, $n = 11$ slices, vs. KO-FF:7.6 ± 0.3, $n = 12$ slices, $^{**}P < 0.01$). (*I–J*) Train with 400 pulses at 33 Hz. (*J*) Last 50 pulses of the train, averaged and depicted as bar diagrams (WT:1.7 ± 0.2, $n = 10$ slices, vs. KO:2.3 ± 0.2, $n = 12$, $^{*}P < 0.05$).

S5). As Stn2 has been shown to stimulate Syt1 internalization when overexpressed in fibroblasts (22), we next probed the levels of surface-stranded Syt1 in hippocampal slices from WT and Stn2 KO mice. To this aim, we applied antibodies that specifically recognize the luminal domain of Syt1 without prior membrane permeabilization. Elevated levels of surface-stranded Syt1 were detected in slices from Stn2 KO mice compared with WT littermates (Fig. 2 *D* and *E*). This defect was specific for Syt1 as the surface levels of Syp, another prominent SV protein, were unaltered (Fig. 2 *F* and *G*). These data suggest that loss of Stn2 selectively alters the partitioning of Syt1 between internal vesicular and surface pools, presumably due to defective sorting of Syt1 but not Syp.

Selective Defect in Endocytic Sorting of Syt1 but Not Synaptophysin or Synaptobrevin 2 in the Absence of Stn2. To directly probe whether the defects in Syt1 distribution observed in vivo reflect a

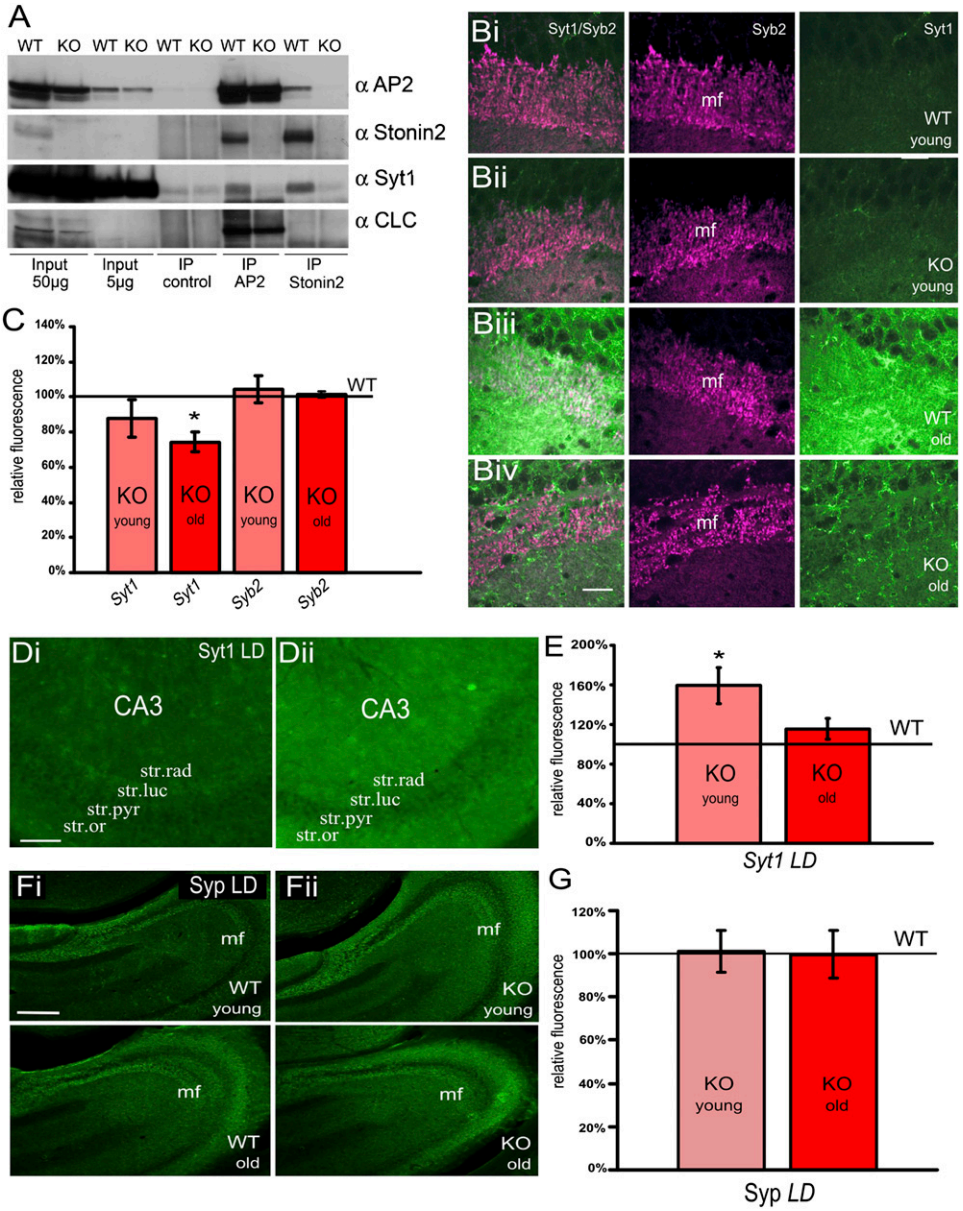

Fig. 2. Repartitioning of Syt1 to the neuronal surface in Stn2 KO brains. (*A*) AP-2 does not coimmunoprecipitate Syt1 in the absence of Stn2. Brain lysates of WT and KO mice were immunoprecipitated with either AP-2 or Stn2 antibody (control, preimmune serum) and analyzed by immunoblotting for AP-2, Stn2, Syt1, and clathrin light chain (CLC). (*B*) Syt1 levels in the hippocampus of young and old WT (*Bi* and *Biii*) and Stn2 KO (*Bii* and *Biv*) mice. Representative epifluorescent images of horizontal brain sections immunostained with Syt1 (green) and synaptobrevin2 (Syb2) (magenta) antibodies. (Scale bar, 40 μm.) (*C*) Quantification of Syt1 and Syb2 levels in the CA3 *stratum lucidum* of Stn2 KO mice relative to WT levels (black line), nWT/KO = 7, $*P < 0.05$. (*D*) Surface-Syt1 levels in the hippocampus of young WT (*Di*) and KO (*Dii*) mice. Epifluorescent images of representative horizontal brain sections immunostained under nonpermeabilizing conditions with Syt1 luminal domain antibody (Syt1 LD). (Scale bar, 100 μm.) (*E*) Quantification of Syt1 LD levels in CA3 of young and old Stn2 KO mice relative to WT levels (black line) (KO young: 159.28 ± 18.37%, $n = 9$; KO old: 119.8 ± 15.22%, $n = 6$, $*P < 0.05$). All data are given as mean ± SEM. (*F*) Surface synaptophysin (Syp LD) immunolabeling in the hippocampus of young and old WT (*Fi*) and Stn2 KO mice (*Fii*). Representative epifluorescent images of coronal brain sections immunostained under nonpermeabilizing conditions with Syp LD antibodies. (*G*) Quantification of Syp LD levels in the CA3 *stratum lucidum*/*stratum pyramidale* of young and old Stn2 KO mice in relation to WT levels (black line). All data represent mean ± SEM. (Scale bars, 250 μm for all images.)

Syt1-specific sorting phenotype, we used pHluorins, fusions between the luminal domain of SV proteins and a pH-sensitive variant of GFP that undergoes quenching within the acidic SV lumen and is dequenched on exocytic fusion with the plasma membrane (15, 16, 23). A significant elevation of the surface-stranded/total Syt1pHluorin ratio (WT: 19.5 ± 1% vs. KO: 28.2 ± 1.6%, $P < 0.0001$) was observed in neurons from Stn2 KO mice compared with their WT littermates (Fig. 3*A*), similar to what is seen for native endogenous surface Syt1 (Fig. S6 *A* and *B*), whereas the total amount of Syt1 per bouton was unaltered (Fig. S6*C*). This defect was specific for Syt1, as synaptophysin-pHluorin (SypHluorin) or synaptobrevin2-pHluorin (Syb2pHluorin) exhibited identical partitioning between SVs and the neuronal surface in neurons from both genotypes (Fig. 3*A*). Defective Syt1 sorting was a direct consequence of loss of Stn2, as it could be rescued by reexpression of Stn2 in KO neurons (Fig. 3*B*). These results together with the in vivo data from hippocampal sections (cf. Fig. 2) provide

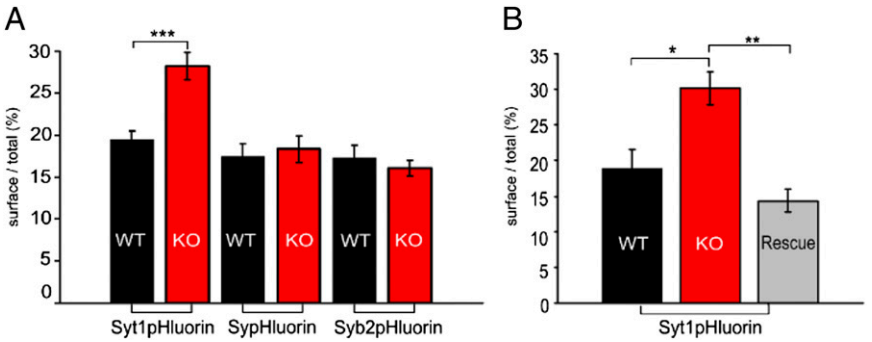

Fig. 3. Selective defect in endocytic sorting of Syt1 but not synaptophysin or synaptobrevin 2 in absence of Stn2. (*A*) Surface-to-total pool ratios of Syt1-, synaptophysin (Syp)-, or synaptobrevin 2 (Syb2)-pHluorin in hippocampal neurons (n = 3 independent experiments, 5–10 coverslips with >50 boutons for each construct and genotype; ***$P < 0.0001$). (*B*) Rescue of defective Syt1 sorting by reexpression of $Stn2^{wt}$ in KO neurons (WT:18.94 ± 2.63%, KO:30.14 ± 2.35%, rescue:14.33 ± 1.59%, *$P < 0.05$, **$P < 0.005$).

direct evidence for the proposal that loss of Stn2 compromises the fidelity of Syt1 sorting.

To obtain further insights into the subsynaptic distribution of surface-stranded Syt1, we analyzed the localization of this surface pool with respect to bassoon, an established marker for AZ membranes, i.e., preferred sites of exocytic SV fusion. Quantitative confocal imaging revealed a significant accumulation of surface Syt1 at bassoon-positive sites in Stn2 KO neurons (Fig. 4 *A* and *B*). Similar to the results from cultured hippocampal neurons, Syt1 was partially redistributed to the surface of MF synapses in vivo (Fig. 4*C*). These data suggest that Stn2 may operate directly at or close to AZ release sites to remove exocytosed Syt1 molecules and to thereby maintain the fidelity of SV protein sorting.

Accelerated SV Retrieval in the Absence of Stn2. SV pool size is regulated at least in part by the balance between exocytic membrane fusion and endocytic SV recycling. To test whether possible alterations in SV cycling may underlie the increase in SV pool size, we followed SV exo-endocytosis using pHluorin-tagged

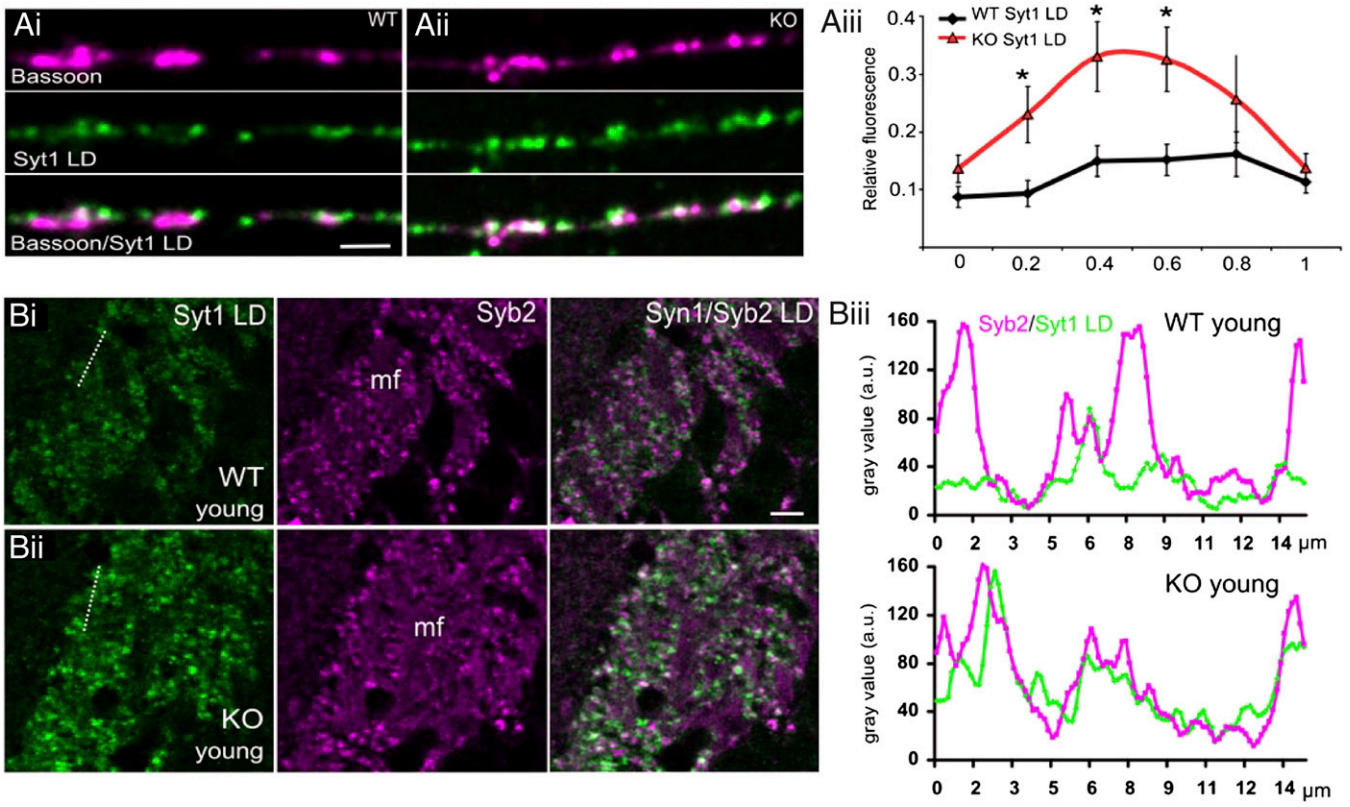

Fig. 4. Accumulation of surface Syt1 within the presynaptic boutons in absence of Stn2. (*A*) Colocalization of Syt1 LD (green) and Bassoon (magenta) in cultured hippocampal neurons from WT (*Ai*) and Stn2 KO mice (*Aii*). (*Aiii*) Distribution pattern of Syt1 LD fluorescence intensity along the Bassoon-positive synaptic bouton in WT (black line) and KO (red line) neurons (two independent experiments, nKO = 28, nWT = 31, synaptic boutons = 50 each, *$P < 0.05$). (Scale bar, 10 µm.) All data are given as mean ± SEM. (*B*) Confocal images of MF synapses from young WT (*Bi*) and Stn2 KO (*Bii*) mice immunostained with Syt1 LD (green) and Syb2 antibodies (magenta). (Scale bar, 8 µm.) (*Biii*) Intensity profiles of Syt1 LD (green) and Syb2 (magenta) fluorescence (measured along dotted lines indicated in *Bi* and *Bii*) illustrate the accumulation of surface-Syt1 within synaptic boutons of KO MF synapses.

SV proteins. Stimulation of WT neurons expressing SypHluorin with a 40-Hz high-frequency pulse for 5 s elicited exo-endocytosis with an apparent time constant of endocytic recovery of about 39 s. Surprisingly and in contrast to any other endocytic protein mutant studied thus far, retrieval of SypHluorin was significantly facilitated in Stn2 KO neurons as evidenced by a shorter apparent time constant (τKO = 29.83 ± 1.94 s) than in WT (τWT = 39.02 ± 2.44 s; Fig. 5*A*). Similar results were obtained in neurons expressing Syt1pHluorin (Fig. 5*A*), indicating that the increased speed of SV protein retrieval was independent from the pHluorin sensor used. Faster retrieval in Stn2 KO neurons was not an indirect consequence of developmental changes, but a direct consequence of loss of Stn2, as it could be fully rescued by reexpression of Stn2 in KO neurons (Fig. 5*Aii*). Facilitated SV retrieval in the absence of Stn2 is consistent with the increased SV pool size observed by electron microscopy analysis of MF boutons and suggests a defect in exo-endocytic balance in Stn2 KO mice.

Repartitioning of Syt1 to the Neuronal Surface Accelerates SV Protein Retrieval. Recent data indicate that Syt1 regulates both exocytosis and endocytosis of SVs at synapses (40, 41). Furthermore, the pool of surface-stranded SV proteins can serve as a substrate for endocytic or endosomal SV reformation (15, 16). It is therefore possible that selective repartitioning and accumulation of non-internalized Syt1 on the surface of synaptic boutons from Stn2 KO neurons may alter the kinetics of SV retrieval in absence of Stn2 (cf. Fig. 5*A*). If this was correct, then overexpression of internalization-defective mutants of Syt1 should mimic the endocytic phenotype observed in Stn2 KO neurons. To probe this, we analyzed SV exo-endocytosis in WT neurons overexpressing $Syt1^{wt}$ or Stn2 binding-defective mutant $Syt1^{mut}$ (23). Indeed, SV retrieval was significantly facilitated in WT neurons overex-

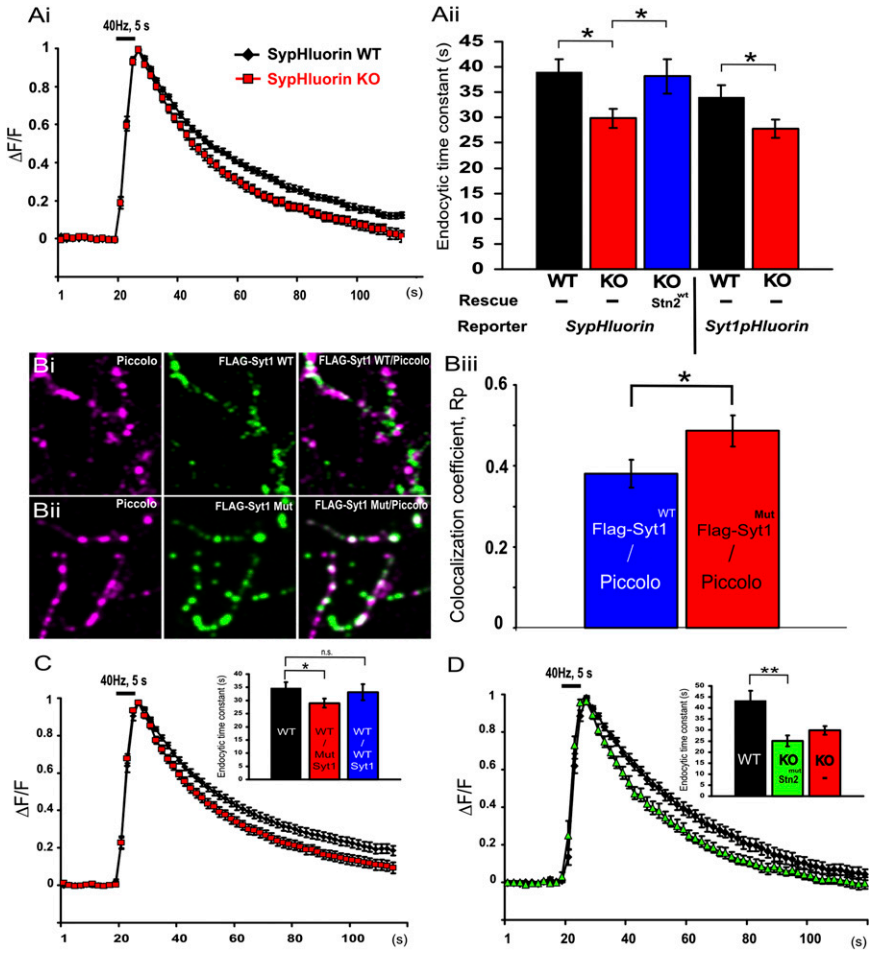

Fig. 5. Syt1 accumulation at the neuronal surface accelerates SV retrieval. (*A*) SV retrieval kinetics in WT and Stn2 KO neurons by recording SypHluorin or Syt1-pHluorin fluorescence during and after field stimulation applied at 40 Hz for 5 s. (*Ai*) Time course of ΔF. (*Aii*) Decay constants from WT and Stn2 KO neurons obtained by monoexponential fit [$f(x) = A_1e^{-x/t1} + y_0$]. τWT = 39.02 ± 2.44 s, τKO = 29.83 ± 1.94 s, $^*P < 0.05$, mean ± SEM of two independent experiments, >700 boutons per genotype. Facilitated retrieval is rescued by reexpression of $Stn2^{WT}$ in KO neurons (τKO + $Stn2^{WT}$ = 38.16 ± 3.41 s, $^*P < 0.05$, mean ± SEM; $n = 3$ independent experiments, >500 boutons per genotype). (*B*) Overexpression of $Syt1^{WT}$ (*Bi*) or Stn2 binding-defective mutant $Syt1^{mut}$ (*Bii*) in WT neurons. Synapses were identified by the AZ marker piccolo (purple), surface Syt1 was visualized with α-FLAG antibodies (green). (Scale bar, 5 μm.) (*Biii*) Surface-stranded Stn2 binding-defective $Syt1^{mut}$ displays significantly elevated levels of colocalization with the AZ marker piccolo (Rp = 0.48 ± 0.038) compared with $Syt1^{WT}$ (Rp = 0.38 ± 0.034, $^*P < 0.05$, mean ± SEM of two independent experiments, >700 boutons per genotype). (*C*) SypHluorin retrieval in control WT neurons (black line, black bar) and neurons overexpressing $Syt1^{WT}$ (blue bar) or Stn2 binding-defective $Syt1^{mut}$ (red line, red bar). Overexpression of $Syt1^{mut}$ (τWT = 34.69 ± 2.23 s, τWT + $Syt1^{mut}$ = 28.99 ± 1.70 s, $^*P < 0.05$, mean ± SEM of four independent experiments, >1,000 boutons per condition) but not $Syt1^{WT}$ (τWT + $Syt1^{wt}$ = 33.17 ± 3.04 s, mean ± SEM of three independent experiments, >700 boutons per condition) facilitates poststimulation fluorescence decay. (*D*) Overexpression of Syt1 binding–defective mutant $Stn2^{\delta KYE}$ in Stn2 KO neurons (green line, green bar) fails to rescue altered SV retrieval (red bar) (τWT = 43.37 ± 4.44 s, τKO + $Stn2^{\delta KYE}$ = 25.10 ± 2.52 s, $^{**}P < 0.005$, mean ± SEM of four independent experiments, ≥300 boutons per condition).

pressing mutant Syt1^{mut} compared with control neurons or to neurons expressing Syt1^{wt} (τWT = 34.69 ± 2.23 s, τWT + Syt1^{mut} = 28.99 ± 1.70 s, τWT + Syt1^{wt} = 33.17 ± 3.04 s; $P < 0.05$; Fig. 5*C*). Moreover, surface-stranded Stn2 binding–defective Syt1^{mut} showed a significantly higher degree of colocalization with the AZ marker piccolo than its WT counterpart (Fig. 5*B*), similar to what is observed for endogenous Syt1 in Stn2 KO neurons. Facilitated SV retrieval is also seen in neurons overexpressing a Syt1 chimera retargeted to the neuronal surface (Syt1-GAP43) (42) (Fig. S7*B*). Finally, an Stn2 mutant, impaired in its ability to interact with Syt1 (Stn2^{mut}) (23) unlike its WT counterpart, failed to rescue the endocytic time constant in KO neurons (Fig. 5*D*). Taken together, these results indicate that facilitated SV protein retrieval in Stn2 KO neurons is a consequence of the selective repartitioning and accumulation of noninternalized Syt1 on the surface of synaptic boutons of Stn2 KO mice.

Facilitated SV Reformation from Endosomes in Stn2 KO Mice. To unravel potential mechanisms underlying facilitated SV protein retrieval in the absence of Stn2, we probed SV exo-endocytosis with different stimulation paradigms. Although SV retrieval in response to a brief 5-s high-frequency pulse at 40 Hz was facilitated (Fig. 5), normal kinetics of SV endocytosis were observed if synapses were challenged with 40 APs applied at 20 Hz (Fig. S7*A*). Because high-frequency stimulation is known to trigger AP-1–mediated SV reformation from bulk endosomes (9, 10), we examined the localization of the endosomal clathrin adaptor complex AP-1 in neurons from WT or Stn2 KO mice. We observed a significant increase in the levels of AP-1 (Fig. 6 *A*–*C*) and in its localization to presynaptic sites (Fig. 6*D*) in stimulated neurons derived from Stn2 KO mice. AP-1 recruitment to membranes depends on Arf and is inhibited by the fungal metabolite brefeldin A (BFA). To determine a potential contribution of AP-1 to SV reformation, we analyzed SV exo-endocytosis induced by brief high-frequency stimulation in WT or Stn2 KO neurons in the presence of BFA. Application of BFA slowed SV retrieval kinetics and, most importantly, eliminated the differences between neurons from both genotypes (Fig. 6*E*). These data indicate that accelerated SV retrieval in Stn2 KO mice may be due, at least in part, to up-regulation of BFA-sensitive SV reformation from bulk endosomes, presumably via AP-1.

Loss of neuronal AP-1 function has been shown to cause the accumulation of bulk endosomes at presynaptic sites, indicating that AP-1 mediates SV reformation from such endosomes (9). If up-regulation of SV reformation from endosomes via AP-1 underlies the elevated SV pool size and accelerated SV retrieval kinetics in the absence of Stn2, one would expect to observe morphological changes in the number and size of bulk endosomes opposite to those seen in AP-1 mutant mice, i.e., a reduced number and size of endosomal structures. Morphometric analyses of Stn2-deficient hippocampal boutons challenged with brief high-frequency stimulation revealed a profound decrease in the number and size of endosomes compared with those from WT littermates (Fig. 6 *H* and *I*), whereas the SV pool size was increased (Fig. 6*G*), similar to what is observed at hippocampal MF boutons in situ (Fig. 1 *A*–*C*). These results are consistent with facilitated SV reformation from endosomes via a BFA-sensitive pathway, and this might underlie the elevated SV pool size and accelerated SV retrieval kinetics in the absence of Stn2.

In summary, our collective data indicate that the absence of Stn2 compromises the fidelity of Syt1 sorting, whereas Stn2 is dispensable for maintaining the speed of SV protein retrieval. Our data are further consistent with a model according to which SV reformation from bulk endosomes supports maintenance of the speed and efficacy of SV reformation but is unable to maintain the compositional identity of SVs, resulting in impaired synaptic function in vivo.

Discussion

The precise mechanisms of SV reformation and protein sorting during successive rounds of SV exo-endocytic cycling have remained a matter of debate (2, 4, 5, 10, 14–16, 43). Mutants lacking key endocytic or endosomal proteins studied thus far exhibit generalized defects in synaptic ultrastructure including a reduced SV pool size and the accumulation of endocytic and endosomal intermediates, often paired with a reduced rate of SV membrane retrieval (4, 21, 25, 32, 44–46). Clearly, such alterations would obscure a potential role of endocytic adaptors as specific sorters for select SV proteins.

Our results reported here demonstrate a cargo-selective function for Stn2 in the retrieval of Syt1 from the neuronal surface at and around AZ membranes (Figs. 2–4), contrary to recent claims (26) and different from invertebrate stonins (27, 29, 31). This statement is evident from the accumulation of endogenous Syt1 at the surface of Stn2-deficient synapses in the hippocampus and in hippocampal neurons in culture (Figs. 2 and 4; Fig. S6), whereas Syp was distributed normally. The Syt1 specificity of this sorting defect in the absence of Stn2 was further confirmed by quantitative analysis of the vesicular-to-surface pool ratio of major SV proteins (Fig. 3).

Several conclusions can be drawn from our study. First, we provide evidence that Stn2 is required for proper sorting of Syt1, whereas it is dispensable for maintaining the kinetics of SV retrieval (schematically depicted in Fig. S8). Our data demonstrate that repartitioning of Syt1 to the neuronal surface in Stn2 KO neurons or overexpression of surface-targeted mutants of Syt1 surprisingly results in an increased rate of SV protein retrieval assessed by pHluorin reporters (Fig. 5). Facilitated SV retrieval (Fig. 1 *D*–*H*), together with a presumably reduced release probability (Fig. 1 *D*–*J*), conforms with and can explain the increase in SV pool size at MF terminals (Fig. 1 *A*–*C*) and at active hippocampal synapses in culture (Fig. 6*G*). Second, our data suggest that loss of Stn2, presumably via repartitioning of Syt1 to neuronal AZ membranes, induces compensatory AP-1–mediated SV reformation from bulk endosomes (Fig. 6). The underlying mechanism that triggers bulk endocytosis is unknown but may involve Syt1-mediated recruitment of adaptors (i.e., AP-1) and/or membrane deforming proteins. Importantly, it appears that SV regeneration by bulk endocytosis is unable to correct sorting defects caused by the absence of Stn2 (Fig. S8). Increased bulk endocytosis and endosomal SV reformation may underlie the observed accelerated kinetics of SV protein retrieval, although other mechanisms, such as bypassing an otherwise rate-limiting step of Syt1 sorting, cannot be ruled out. Our observations fit with earlier data indicating that bulk endocytosis and endosomal SV reformation are primarily induced by high-frequency stimulation, conditions under which refilling of the SV pool may become rate limiting for proper neurotransmission. Thus, maintenance of the speed of neurotransmission by SV reformation from bulk endosomes may come at the price of compromised sorting fidelity. Third, the observation that loss of Stn2 in mice causes specific missorting of Syt1 but not other SV proteins supports the notion that SVs, at least over multiple exo-endocytic cycles, lose their identity (15, 16, 47) and are reassembled from the pool of surface-stranded SV proteins. Endocytic sorting and reassembly of SV proteins presumably involve the cooperation of multiple endocytic adaptors including Stn2 (this study), AP180/CALM (18, 19, 48), and likely others via clathrin/AP-2–mediated endocytosis. Hence, neurons appear to have evolved distinct pathways for SV reformation to balance sorting fidelity (i.e., via Stn2 and AP180) with the speed of SV exo-endocytosis.

Our data agree with and explain the established evolutionary conserved role of Syt1 as a facilitator of SV membrane retrieval in mice (41), flies (49, 50), and worms (51). Sustained genetic

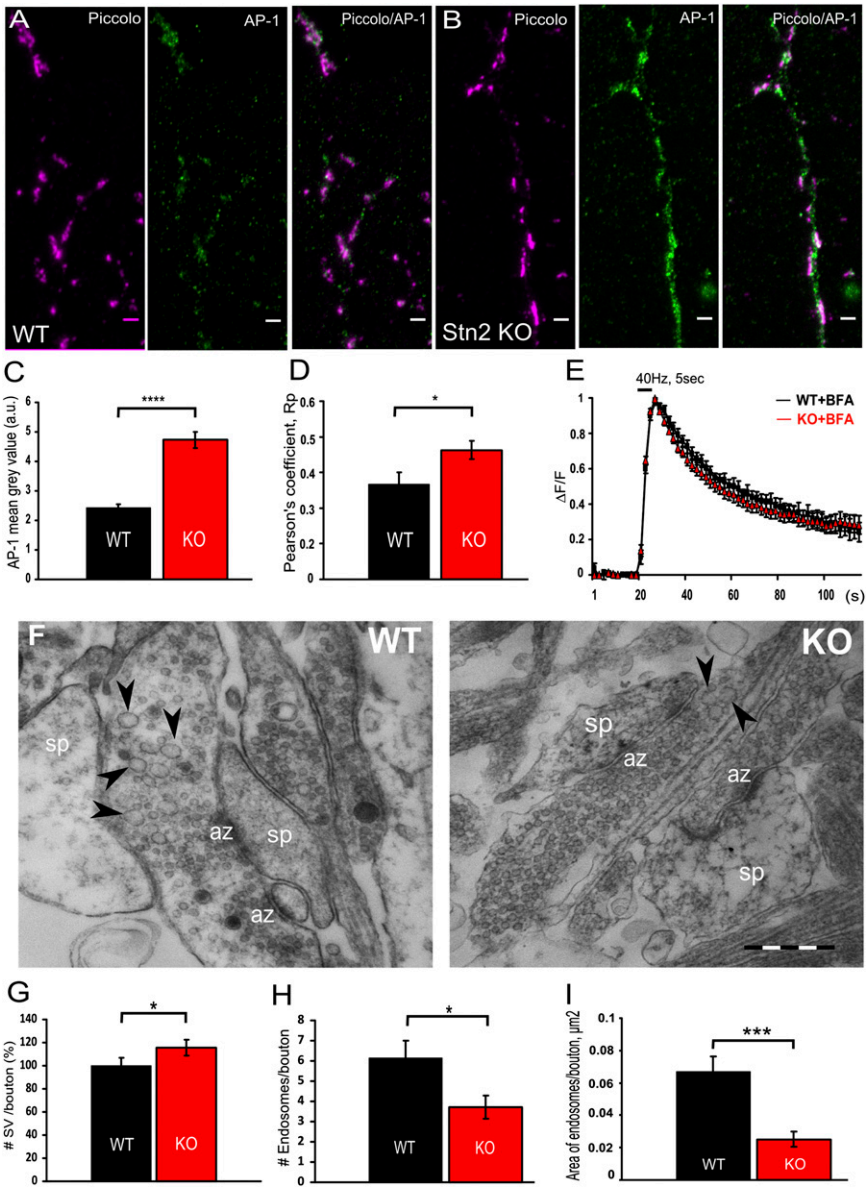

Fig. 6. Facilitated SV reformation from endosomes in Stn2 KO mice. (*A–D*) Accumulation of AP-1 at synaptic boutons of cultured Stn2 KO neurons stimulated with 200 APs at 40 Hz. Representative epifluorescent images of cultured hippocampal neurons from WT (*A*) and Stn2 KO (*B*) mice immunostained for the AZ marker piccolo (magenta) and AP-1 (green). (Scale bar, 1 μm.) (*C*) Elevated levels of AP-1 (i.e., mean gray value) in stimulated neurons from Stn2 KO mice (4.727 ± 0.264) compared with WT littermates (2.423 ± 0.132). ****$P < 0.000000005$, mean ± SEM, ≥600 boutons per condition. (*D*) Increased accumulation of AP-1 at piccolo-containing presynaptic AZs in Stn2 KO neurons (Rp = 0.463 ± 0.025) compared with WT neurons (Rp = 0.366 ± 0.033, *$P < 0.05$, mean ± SEM, ≥600 boutons per condition). (*E*) Effects of brefeldin A (BFA) on SV exo-endocytosis. Endocytic poststimulation fluorescent decay of Syt1-pHluorin is similar in BFA-treated neurons from Stn2 KO (35.82 ± 4.94) compared with WT mice (37.60 ± 5.61). Time course of ΔF (data point fluorescence-resting fluorescence) was normalized to the peak value (*F*peak). Mean ± SEM of three independent experiments, >1,000 boutons per condition. (*F*) Electron microscopic images of hippocampal boutons from cultured WT or Stn2 KO neurons stimulated with 200 APs at 40 Hz: sp, spine; az, active zone; black arrows, endosomal structures. (Scale bar, 1 μm.) (*G*) Mean SV density in cultured Stn2 KO synapses is significantly higher (116 ± 6.93%) compared with WT synapses (100 ± 6.71%). Mean vesicle density in KO synapses normalized to WT (40 synapses per genotype, *$P < 0.05$). (Scale bar, 1 μm.) (*H*) The number of endosomes is significantly decreased in Stn2 KO neurons (3.81 ± 0.58) compared with WT neurons (6.14 ± 0.86). Mean ± SEM, 40 synapses per genotype, *$P < 0.05$. (*I*) The membrane area of endosomal structures in Stn2 KO neurons is significantly smaller (0.025 ± 0.004 μm^2) compared with WT neurons (0.066 ± 0.009 μm^2). Mean ± SEM, 40 synapses per genotype, ***$P < 0.0005$.

(41, 51, 52) or acute inactivation of Syt1 function (50) in vivo results in a reduced rate of SV endocytosis, a phenotype opposite to that observed in Stn2 KO neurons, where Syt1 accumulates on the surface of synaptic boutons. Selective Stn2-mediated Syt1 retrieval from release sites might thus contribute to exo-endocytic coupling (6, 41).

The fact that Stn2 KO mice are viable and able to internalize Syt1, albeit with a reduced fidelity of sorting, indicates that, unlike in invertebrates where stonins constitute an essential component of the machinery for SV retrieval (27–29, 31), compensatory mechanisms must exist in mammalian synapses. Our data suggest that such compensation may be achieved at least in part via up-regulation of an AP-1–mediated bulk endosomal pathway of SV reformation (Fig. 6). However, it cannot be ruled out that other, yet to be identified pathways or components of the mammalian endocytic machinery functionally overlap with

Stn2. For example, earlier biochemical (39) and genetic data have implicated a tight functional coupling between Syt1 and the SV2 family of SV membrane proteins (53). SV2 associates with endocytic proteins including AP-2 and Eps15 (39, 53), and loss of SV2A/B in mice is associated with defects in Syt1 sorting and in neurotransmission (53). No close SV2 homologs have been identified in invertebrates, suggesting that SV2 A/B might fulfill a vertebrate-specific role in Syt1 exo-endocytic cycling. Whether SV2 and Stn2 are components of a unique common mechanism for Syt1 endocytosis or operate via different pathways remains to be determined. A similar model has recently been proposed for the SV SNARE Syb2, which is recognized by its specific endocytic adaptors AP180 and CALM (19), but in addition requires Syp for efficient exo-endocytosis in vivo (54, 55).

Syt1 repartitioning to the neuronal surface and impaired short-term plasticity at mossy fiber synapses in Stn2 KO mice are associated with behavioral alterations in these animals, in particular with increased exploration-related behaviors. These alterations resemble arousal seeking and impulsivity observed in patients suffering from Tourette syndrome (35) or schizophrenia (36). Recent data from human genetics have indeed revealed a possible association of Stn2 with such neuropsychiatric disorders including schizophrenia and autism-spectrum disorders (37, 38). Hence, the work reported here could serve as a starting point for the dissection of the molecular mechanisms underlying these neuropsychiatric disorders.

Materials and Methods

Generation of Stn2 KO Mice. The mouse Stn2 gene is located on chromosome 12 and consists of seven exons. Exon 5 harbors about 70% of the coding sequence (CDS), allowing for targeted deletion of the majority of the Stn2 CDS. We designed a targeting vector containing a neomycin cassette flanked on one site by a 1.6-kb genomic sequence homologous to the upstream region of exon 5 and on the other site by a 7.3-kb genomic sequence comprising the end of exon 5 and the downstream intronic sequence (Fig. S2*A*). This construct was electroporated into ES14 mouse embryonic stem cells. ES cell clones were injected into C57 BL/6 blastocysts and subsequently implanted into pseudopregnant mice. The resulting chimeric males were mated with C57 BL/6 females to yield heterozygous Stn2 KO mice, which were backcrossed with C57 BL/6 J mice for 15 generations to obtain a congenic line. Heterozygous Stn2 KO mice did not show any overt phenotypic differences to WT animals and were interbred to obtain Stn2 WT and KO littermates for experiments.

pHluorin Imaging of Living Neurons. Hippocampal neurons, including granule neurons of dentate gyrus, from neonatal mouse brain (P3–P6) were prepared in a sparse culture according to previously described protocols with minor modifications (47, 56) and transfected at DIV (days in vitro) 6–8 by a modified calcium phosphate transfection procedure (57, 58). Imaging was performed at 12–16 DIV essentially as described (22, 59). Neurons were subjected to electrical field stimulation at 40 Hz for 5 s using an RC-21B stimulation chamber (Warner Instruments) and imaged at room temperature in basic buffer [170 mM NaCl, 3.5 mM KCl, 0.4 mM KH_2PO_4, 20 mM *N*-Tris[hydroxy-methyl]-methyl-2-aminoethane-sulphonic acid (TES), 5 mM $NaHCO_3$, 5 mM glucose, 1.2 mM Na_2SO_4, 1.2 mM $MgCl_2$, 1.3 mM $CaCl_2$, 10 μM CNQX, and 50 μM AP-5, pH 7.4] using an inverted Zeiss Axiovert 200M microscope with a 40× oil-immersion objective, eGFP filter set (BP 525–50), and CCD camera. To measure the total fluorescence (*F*out), 50 mM NaCl was replaced by NH_4Cl, and to dequench the surface fraction of the probes (*F*in), TES was substituted by (2-(*N*-morpholino)ethanesulfonic acid) (Mes) (pH 5.5). The fraction of plasma membrane-stranded pHluorin was calculated as *F*out/(*F*out + *F*in). Images were collected every 2 s in experiments involving stimulation and every 5 s for the measurement of the surface-stranded pool of SV proteins. Quantitative analysis was performed with Slidebook software (Inovision). For kinetics analysis, the time course of ΔF [F (data point fluorescence) – $F0$ (resting fluorescence)] was normalized with respect to the peak value (*F*peak). Poststimulation time constants were determined by fitting the monoexponential decay curve [$y_0 + A^*\exp(-x/t)$] using QtiPlot software (http://soft.proindependent.com/qtiplot.html). Brefeldin-A was obtained from Sigma and used at 10 μg/mL where indicated.

Electrophysiological Recordings. Mice (3–6 mo old) were decapitated under deep isoflurane anesthesia, and the brains were quickly removed and cooled down in ice-cold sucrose-based artificial cerebrospinal fluid (sACSF; in mM): 50 NaCl, 1 NaH_2PO_4, 2.5 KCl, 25 $NaHCO_3$, 7 $MgCl_2$, 0.5 $CaCl_2$, 150 sucrose, and 10 glucose. Brain slices (300 μm thick) were cut with a vibratome (VT1200S; Leica) and stored in a slice chamber with sACSF. After a 30-min incubation at 36–37 °C, slices were transferred to physiological ACSF solution (containing in mM: 124 NaCl, 1.25 NaH_2PO_4, 3 KCl, 1.3 $MgSO_4$, 2.5 $CaCl_2$, 26 $NaHCO_3$, and 10 glucose, saturated with 95% O_2/5% CO_2 at a pH of 7.4). Field excitatory postsynaptic potential (fEPSP) recordings were performed with low-resistance patch pipettes using a MultiClamp 700B amplifier (Axon Instruments). The stimulation electrode was placed in the hilus of the dentate gyrus, and field potentials were recorded in *stratum lucidum* of CA3. At the beginning of every recording, the frequency facilitation protocol (1 Hz) was applied (60), and the experiment was only continued if the fEPSP increase seen was >400%. At the end of every experiment, application of the group II mGluR agonist DCG-IV (1 μM) was used to verify that pure mossy fiber responses were recorded. Experiments were only included if the reduction was >90% of baseline amplitude. Data filtered at 2 kHz and digitized (BNC-2090; National Instruments) at 5 kHz were analyzed with custom-made software in IGOR Pro (WaveMetrics).

Statistical Analysis. The statistical significance for all data except immunostaining on brain sections and electrophysiological recordings was evaluated with a two-tailed paired Student *t* test. Differences in fluorescence intensity of immunostained proteins between WT and Stn2KO littermates were statistically tested with the paired Wilcoxon signed rank sum test. Analysis of electrophysiological data was performed via an unpaired two-tailed Student *t* test. Significant differences were accepted at $P < 0.05$.

ACKNOWLEDGMENTS. We thank Dr. Reinhard Jahn (MPI Göttingen) for antibodies and Sabine Hahn, Ingeborg Walther, and Antje Grünwald for technical assistance. This work was supported by grants from the Deutsche Forschungsgemeinschaft (DFG) (SFB958/ A01; HA2686/1-3; Exc 257-Neurocure) and the European Science Foundation.

1. Jahn R, Scheller RH (2006) SNAREs—Engines for membrane fusion. *Nat Rev Mol Cell Biol* 7(9):631–643.
2. Sudhof TC (2004) The synaptic vesicle cycle. *Annu Rev Neurosci* 27:509–547.
3. Galli T, Haucke V (2004) Cycling of synaptic vesicles: How far? How fast! *Sci STKE* 2004 (264):re19.
4. Dittman J, Ryan TA (2009) Molecular circuitry of endocytosis at nerve terminals. *Annu Rev Cell Dev Biol* 25:133–160.
5. Murthy VN, De Camilli P (2003) Cell biology of the presynaptic terminal. *Annu Rev Neurosci* 26:701–728.
6. Haucke V, Neher E, Sigrist SJ (2011) Protein scaffolds in the coupling of synaptic exocytosis and endocytosis. *Nat Rev Neurosci* 12(3):127–138.
7. Hoopmann P, et al. (2010) Endosomal sorting of readily releasable synaptic vesicles. *Proc Natl Acad Sci USA* 107(44):19055–19060.
8. Voglmaier SM, et al. (2006) Distinct endocytic pathways control the rate and extent of synaptic vesicle protein recycling. *Neuron* 51(1):71–84.
9. Glyvuk N, et al. (2010) AP-1/sigma1B-adaptin mediates endosomal synaptic vesicle recycling, learning and memory. *EMBO J* 29(8):1318–1330.
10. Cheung G, Cousin MA (2012) Adaptor protein complexes 1 and 3 are essential for generation of synaptic vesicles from activity-dependent bulk endosomes. *J Neurosci* 32(17):6014–6023.
11. Takamori S, et al. (2006) Molecular anatomy of a trafficking organelle. *Cell* 127(4): 831–846.
12. Mutch SA, et al. (2011) Protein quantification at the single vesicle level reveals that a subset of synaptic vesicle proteins are trafficked with high precision. *J Neurosci* 31 (4):1461–1470.
13. Willig KI, Rizzoli SO, Westphal V, Jahn R, Hell SW (2006) STED microscopy reveals that synaptotagmin remains clustered after synaptic vesicle exocytosis. *Nature* 440(7086): 935–939.
14. Opazo F, et al. (2010) Limited intermixing of synaptic vesicle components upon vesicle recycling. *Traffic* 11(6):800–812.
15. Fernández-Alfonso T, Kwan R, Ryan TA (2006) Synaptic vesicles interchange their membrane proteins with a large surface reservoir during recycling. *Neuron* 51(2): 179–186.
16. Hua Y, et al. (2011) A readily retrievable pool of synaptic vesicles. *Nat Neurosci* 14(7): 833–839.
17. Traub LM (2009) Tickets to ride: Selecting cargo for clathrin-regulated internalization. *Nat Rev Mol Cell Biol* 10(9):583–596.
18. Bao H, et al. (2005) AP180 maintains the distribution of synaptic and vesicle proteins in the nerve terminal and indirectly regulates the efficacy of Ca2+-triggered exocytosis. *J Neurophysiol* 94(3):1888–1903.

19. Koo SJ, et al. (2011) SNARE motif-mediated sorting of synaptobrevin by the endocytic adaptors clathrin assembly lymphoid myeloid leukemia (CALM) and AP180 at synapses. *Proc Natl Acad Sci USA* 108(33):13540–13545.
20. Nonet ML, et al. (1999) UNC-11, a Caenorhabditis elegans AP180 homologue, regulates the size and protein composition of synaptic vesicles. *Mol Biol Cell* 10(7): 2343–2360.
21. Milosevic I, et al. (2011) Recruitment of endophilin to clathrin-coated pit necks is required for efficient vesicle uncoating after fission. *Neuron* 72(4):587–601.
22. Diril MK, Wienisch M, Jung N, Klingauf J, Haucke V (2006) Stonin 2 is an AP-2-dependent endocytic sorting adaptor for synaptotagmin internalization and recycling. *Dev Cell* 10(2):233–244.
23. Jung N, et al. (2007) Molecular basis of synaptic vesicle cargo recognition by the endocytic sorting adaptor stonin 2. *J Cell Biol* 179(7):1497–1510.
24. Maritzen T, Podufall J, Haucke V (2010) Stonins—specialized adaptors for synaptic vesicle recycling and beyond? *Traffic* 11(1):8–15.
25. Mitsunari T, et al. (2005) Clathrin adaptor AP-2 is essential for early embryonal development. *Mol Cell Biol* 25(21):9318–9323.
26. Willox AK, Royle SJ (2012) Stonin 2 is a major adaptor protein for clathrin-mediated synaptic vesicle retrieval. *Curr Biol* 22(15):1435–1439.
27. Fergestad T, Davis WS, Broadie K (1999) The stoned proteins regulate synaptic vesicle recycling in the presynaptic terminal. *J Neurosci* 19(14):5847–5860.
28. Phillips AM, Ramaswami M, Kelly LE (2010) Stoned. *Traffic* 11(1):16–24.
29. Stimson DT, et al. (2001) Drosophila stoned proteins regulate the rate and fidelity of synaptic vesicle internalization. *J Neurosci* 21(9):3034–3044.
30. Stimson DT, Estes PS, Smith M, Kelly LE, Ramaswami M (1998) A product of the Drosophila stoned locus regulates neurotransmitter release. *J Neurosci* 18(23): 9638–9649.
31. Mullen GP, et al. (2012) UNC-41/stonin functions with AP2 to recycle synaptic vesicles in Caenorhabditis elegans. *PLoS ONE* 7(7):e40095.
32. Ferguson SM, et al. (2007) A selective activity-dependent requirement for dynamin 1 in synaptic vesicle endocytosis. *Science* 316(5824):570–574.
33. Voss JL, Gonsalves BD, Federmeier KD, Tranel D, Cohen NJ (2011) Hippocampal brain-network coordination during volitional exploratory behavior enhances learning. *Nat Neurosci* 14(1):115–120.
34. Moser EI, Moser MB, Andersen P (1994) Potentiation of dentate synapses initiated by exploratory learning in rats: Dissociation from brain temperature, motor activity, and arousal. *Learn Mem* 1(1):55–73.
35. Palumbo D, Kurlan R (2007) Complex obsessive compulsive and impulsive symptoms in Tourette's syndrome. *Neuropsychiatr Dis Treat* 3(5):687–693.
36. Hoptman MJ, et al. (2004) DTI and impulsivity in schizophrenia: A first voxelwise correlational analysis. *Neuroreport* 15(16):2467–2470.
37. Breedveld GJ, Fabbrini G, Oostra BA, Berardelli A, Bonifati V (2010) Tourette disorder spectrum maps to chromosome 14q31.1 in an Italian kindred. *Neurogenetics* 11(4): 417–423.
38. Luan Z, et al. (2011) Positive association of the human STON2 gene with schizophrenia. *Neuroreport* 22(6):288–293.
39. Haucke V, De Camilli P (1999) AP-2 recruitment to synaptotagmin stimulated by tyrosine-based endocytic motifs. *Science* 285(5431):1268–1271.
40. Yao J, Kwon SE, Gaffaney JD, Dunning FM, Chapman ER (2012) Uncoupling the roles of synaptotagmin I during endo- and exocytosis of synaptic vesicles. *Nat Neurosci* 15(2):243–249.
41. Nicholson-Tomishima K, Ryan TA (2004) Kinetic efficiency of endocytosis at mammalian CNS synapses requires synaptotagmin I. *Proc Natl Acad Sci USA* 101(47): 16648–16652.
42. Hui E, Johnson CP, Yao J, Dunning FM, Chapman ER (2009) Synaptotagmin-mediated bending of the target membrane is a critical step in Ca(2+)-regulated fusion. *Cell* 138 (4):709–721.
43. Zhang Q, Li Y, Tsien RW (2009) The dynamic control of kiss-and-run and vesicular reuse probed with single nanoparticles. *Science* 323(5920):1448–1453.
44. Wucherpfennig T, Wilsch-Bräuninger M, González-Gaitán M (2003) Role of Drosophila Rab5 during endosomal trafficking at the synapse and evoked neurotransmitter release. *J Cell Biol* 161(3):609–624.
45. Majumdar A, Ramagiri S, Rikhy R (2006) Drosophila homologue of Eps15 is essential for synaptic vesicle recycling. *Exp Cell Res* 312(12):2288–2298.
46. Zhang B, et al. (1998) Synaptic vesicle size and number are regulated by a clathrin adaptor protein required for endocytosis. *Neuron* 21(6):1465–1475.
47. Wienisch M, Klingauf J (2006) Vesicular proteins exocytosed and subsequently retrieved by compensatory endocytosis are nonidentical. *Nat Neurosci* 9(8):1019–1027.
48. Harel A, Wu F, Mattson MP, Morris CM, Yao PJ (2008) Evidence for CALM in directing VAMP2 trafficking. *Traffic* 9(3):417–429.
49. Littleton JT, et al. (2001) synaptotagmin mutants reveal essential functions for the C2B domain in Ca2+-triggered fusion and recycling of synaptic vesicles in vivo. *J Neurosci* 21(5):1421–1433.
50. Poskanzer KE, Marek KW, Sweeney ST, Davis GW (2003) Synaptotagmin I is necessary for compensatory synaptic vesicle endocytosis in vivo. *Nature* 426(6966):559–563.
51. Jorgensen EM, et al. (1995) Defective recycling of synaptic vesicles in synaptotagmin mutants of Caenorhabditis elegans. *Nature* 378(6553):196–199.
52. Poskanzer KE, Fetter RD, Davis GW (2006) Discrete residues in the c(2)b domain of synaptotagmin I independently specify endocytic rate and synaptic vesicle size. *Neuron* 50(1):49–62.
53. Yao J, Nowack A, Kensel-Hammes P, Gardner RG, Bajjalieh SM (2010) Cotrafficking of SV2 and synaptotagmin at the synapse. *J Neurosci* 30(16):5569–5578.
54. Gordon SL, Leube RE, Cousin MA (2011) Synaptophysin is required for synaptobrevin retrieval during synaptic vesicle endocytosis. *J Neurosci* 31(39):14032–14036.
55. Kwon SE, Chapman ER (2011) Synaptophysin regulates the kinetics of synaptic vesicle endocytosis in central neurons. *Neuron* 70(5):847–854.
56. Malgaroli A, Tsien RW (1992) Glutamate-induced long-term potentiation of the frequency of miniature synaptic currents in cultured hippocampal neurons. *Nature* 357(6374):134–139.
57. Threadgill R, Bobb K, Ghosh A (1997) Regulation of dendritic growth and remodeling by Rho, Rac, and Cdc42. *Neuron* 19(3):625–634.
58. Xia Z, Dudek H, Miranti CK, Greenberg ME (1996) Calcium influx via the NMDA receptor induces immediate early gene transcription by a MAP kinase/ERK-dependent mechanism. *J Neurosci* 16(17):5425–5436.
59. Pechstein A, et al. (2010) Regulation of synaptic vesicle recycling by complex formation between intersectin 1 and the clathrin adaptor complex AP2. *Proc Natl Acad Sci USA* 107(9):4206–4211.
60. Gundlfinger A, et al. (2007) Adenosine modulates transmission at the hippocampal mossy fibre synapse via direct inhibition of presynaptic calcium channels. *J Physiol* 582(Pt 1):263–277.